

# Vacuum-free preparation of 7.5% efficient $\text{Cu}_2\text{ZnSn}(\text{S,Se})_4$ solar cells based on metal salt precursors



Thomas Schnabel\*, Manuel Löw, Erik Ahlswede

Zentrum für Sonnenenergie- und Wasserstoff-Forschung, Industriestraße 6, 70565 Stuttgart, Germany

## ARTICLE INFO

### Article history:

Received 20 December 2012

Received in revised form

18 April 2013

Accepted 16 June 2013

### Keywords:

CZTSSe

Earth abundant

Kesterites

Solar cells

Solution processing

## ABSTRACT

A solution-based preparation route for 7.5% efficient thin-film solar cells with a kesterite-type  $\text{Cu}_2\text{ZnSn}(\text{S,Se})_4$  absorber is reported that allows low carbon residues after a rapid selenization step. Metal salts are dissolved in dimethyl sulfoxide and subsequently coated and selenized in a simple process that uses only earth abundant elements. Despite the observation of a layered structure, no clear differences are distinguishable in the chemical composition or phase formation within the absorber layer. However, there is evidence of a ZnSe-rich layer at the molybdenum back contact.

© 2013 Elsevier B.V. All rights reserved.

## 1. Introduction

In the last decade  $\text{CuIn}_{1-x}\text{Ga}_x\text{Se}_2$  (CIGS) and CdTe have gained particular interest as absorber materials in thin film photovoltaic devices with maximum power conversion efficiencies of 20.3 and 17.3%, respectively [1]. But both materials have some disadvantages for large-scale photovoltaic device production because of limited availability of the elements (In, Te) and environmental concerns (Cd). Therefore, the kesterite-type  $\text{Cu}_2\text{ZnSn}(\text{S,Se})_4$  (CZTS(e)) might be a better long-term solution for the fabrication of photovoltaic devices, since all elements are non-toxic and available in high quantities at reasonable prices. Additionally, the material has a high optical absorption coefficient ( $> 1 \times 10^4 \text{ cm}^{-1}$ ) [2] and a direct, tunable band gap (ranging from 0.9 to 1.5 eV) [3,4], that makes it ideal for photovoltaic applications. The techniques for depositing the CZTS (e) absorber layer on the substrate can be divided into two general approaches: vacuum-based deposition, such as sputtering and thermal evaporation, and vacuum-free deposition, such as electrodeposition, spray-pyrolysis and “ink”-based deposition. A good review is given e.g. in Ref. [5,28]. At present, the maximum power conversion efficiency for coevaporated CZTS(e) is 9.15% [6], but the highest obtained efficiency for a kesterite material of 11.1% was reported from a vacuum-free “ink” precursor using hydrazine [7]. For comparison, the highest power conversion efficiency for CIGS was obtained via coevaporation [8].

In this work we report a facile preparation route for a mixed sulfoselenide CZTS(e) device without the use of the highly toxic hydrazine. Owing to low carbon residues and only little Sn loss, high efficiencies well above 7% could be demonstrated. The process is based on an approach reported by Ki et al., that has achieved a power conversion efficiency of 4.1% [9]. Metal salts and thiourea are dissolved in dimethyl sulfoxide (DMSO), afterwards the substrate is coated and selenized. However, we altered the process in manifold aspects to make it simpler and could still reach considerably higher efficiencies at the same time. First of all, we used doctor blading instead of spin coating to demonstrate the potential of the process also for industrial applications and to decrease material consumption. Furthermore, we could lower the drying temperature to 300 °C under nitrogen flow instead of 580 °C in a glovebox. For that purpose and also to improve the wetting behavior, we diluted the DMSO solution with acetone. The process time could be reduced to only a few minutes at the maximum temperature. It is furthermore interesting to note, that although we have a smaller amount of sulfur and hence a smaller band gap of 1.07 eV (compared to 1.15 eV estimated by Ki et al.), our open-circuit voltage of 404 mV is roughly the same. This can be a potential indicator of reduced recombination.

## 2. Experimental

### 2.1. Preparation

The precursor solution was prepared by dissolving copper(II)-acetate monohydrate (99.99%, 2.3 mmol), zinc(II)-chloride (99.995%,

\* Corresponding author. Tel.: +497317870339.

E-mail addresses: [thomas.schnabel@zsw-bw.de](mailto:thomas.schnabel@zsw-bw.de), [thomasschnabel@web.de](mailto:thomasschnabel@web.de) (T. Schnabel).

1.6 mmol), tin(II)-chloride dihydrate (99.995%, 1.6 mmol) and thiourea (99.0%, 7.5 mmol) into 2 ml dimethyl sulfoxide (99.9%, all chemicals from Sigma-Aldrich) by magnetic stirring for several hours at room temperature following a similar route described by Ki et al. [9]. The achieved yellow metal salt solution was diluted with two parts of acetone (99.5%) to improve the wetting behavior.

The precursor solution was deposited onto a Mo-coated soda lime glass ( $76 \times 26 \times 1 \text{ mm}^3$ ) via doctor-blade coating with a Zehntner ZUA 2000. The subsequent drying was performed for 1 min under nitrogen flow at  $300^\circ\text{C}$  on a hot plate. The coating and drying procedure was repeated eight times in order to build up film thickness.

Afterwards, the samples were annealed in Se-containing nitrogen-atmosphere. Two samples, each  $26 \times 76 \text{ mm}^2$  in size, were heated in a graphite box in the presence of approximately 1 g Se pellets, that were arranged around the samples. A simple homemade halogen-lamp-heated furnace was used, which was evacuated and refilled with  $\text{N}_2$  to a process pressure of 50 mbar. No additional Sn was supplied. The annealing temperature of  $540^\circ\text{C}$  was kept constant for approximately six minutes, afterwards the sample was allowed to cool down naturally (a temperature-diagram of the annealing process can be found in the Supporting information). Device fabrication was done by a wet-chemically processed CdS buffer layer, a sputtered ZnO window layer (*i*-ZnO) and a transparent ZnO:Al front-contact to obtain functional solar cells using standard procedures as described in Ref [10].

## 2.2. Characterization

All characterization data were obtained from identical reference samples that were selenized in one process. The Raman measurement was conducted using a WITec CRM 200 with a 532 nm laser source and a spot size of approximately  $1 \mu\text{m}$ . The surface morphology was investigated with a scanning electron microscope (XL30 SFEG Sirion) from FEI Company, using a 5 kV acceleration voltage. For the energy dispersive X-ray (EDX) measurement, an acceleration voltage of 20 kV was applied. Current–voltage curves were measured using a Keithley 238 source measuring unit under simulated AM 1.5 global solar irradiation with an ORIEL sun simulator at  $100 \text{ mW}/\text{cm}^2$  to extract the basic solar-cell characteristics from devices, approximately  $0.24 \text{ cm}^2$  in size. Quantum efficiency measurements were performed using an OptoSolar SR 300 setup. A secondary neutral mass spectrometry (SNMS) analysis was conducted with a Leybold SSM 200 LHS 10 system with a focused 5 keV  $\text{Ar}^+$  ion beam for depth profiling of the composition. Additionally, a Panalytical Empyrean setup was used to perform a grazing incidence X-ray diffraction (GIXRD) measurement.

## 3. Results and discussion

The current–voltage ( $J$ - $V$ ) characteristic is illustrated in Fig. 1a. The characteristic data are an open-circuit voltage of 404 mV, a short-circuit current density of  $29.5 \text{ mA}/\text{cm}^2$ , a fill factor of 62.8% and a total area power conversion efficiency of 7.5%. The sample shows only little shunting and a low series resistance (for details see Fig. 1a). To confirm the sun simulator data, a quantum efficiency measurement was performed (Fig. 1b). The maximum value is 89% (570 nm) and the obtained short circuit current density is  $30.6 \text{ mA}/\text{cm}^2$ , which is in good agreement with the result obtained from the sun simulator. The shoulder at about 470 nm is due to the absorption of the cadmium sulfide buffer layer. A weak decay in the long wavelength region can be indicative of back contact recombination losses or spatial band gap inhomogeneities [7]. In fact, a rather low optical band gap

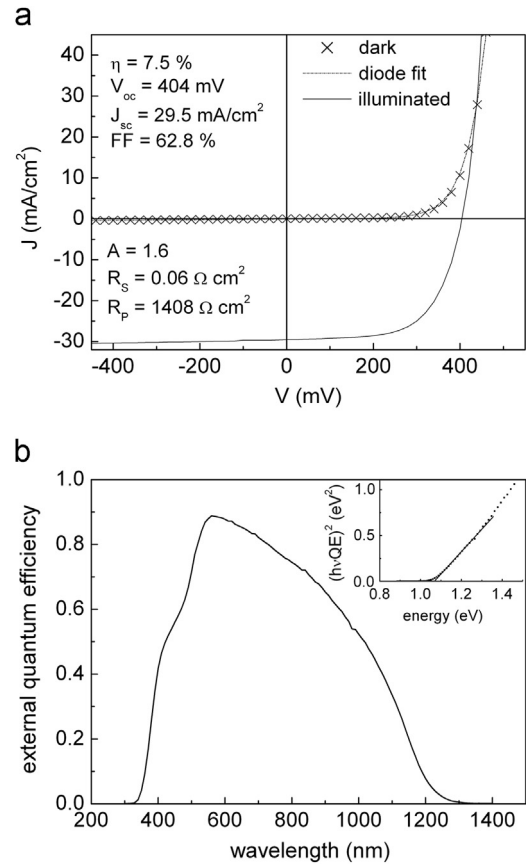


**Fig. 1.** (a) Light and dark  $J$ - $V$  characteristics of the best cell annealed at  $540^\circ\text{C}$ . The fitted values for the diode factor  $A$ , series resistance  $R_s$  and parallel resistance  $R_p$  are also given. (b) External quantum efficiency of the best cell. Inset: Estimation of the band gap via linear extrapolation of the quantum efficiency data.

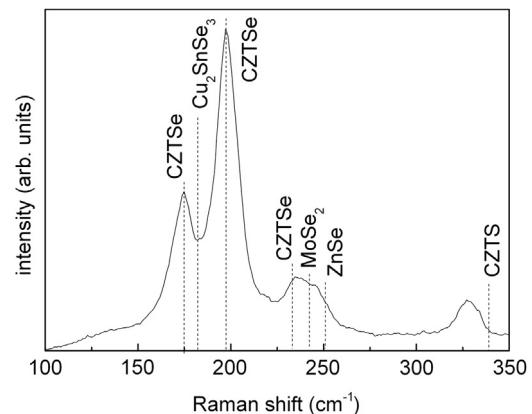


**Fig. 2.** Surface Raman spectrum of a selenized CZTS(e) sample measured at room temperature with an excitation wavelength of 532 nm.

1.07 eV is determined from linear extrapolation of the quantum efficiency data.

The surface Raman spectrum of the sample is shown in Fig. 2. According to [11], the main Raman modes for the kesterite-phase CZTSe are expected at 173, 196 ( $A_1$ -mode) and  $233 \text{ cm}^{-1}$ . These values match quite well with our experimental data. However, the latter peak can also superpose the  $\text{MoSe}_2$  peak at  $242 \text{ cm}^{-1}$  [12], ZnSe at  $253 \text{ cm}^{-1}$  (both formed at the back contact, see discussion below) and  $\text{Cu}_2\text{SnSe}_3$  at  $236 \text{ cm}^{-1}$  [13], so the existence of secondary phases cannot be ruled out. But  $\text{Cu}_2\text{SnSe}_3$  as a ternary

Download English Version:

<https://daneshyari.com/en/article/6536278>

Download Persian Version:

<https://daneshyari.com/article/6536278>

[Daneshyari.com](https://daneshyari.com)